Study of the THGEM detector with a reflective CsI photocathode*

LIU Hong-Bang(刘宏邦)[1,2;1)] ZHENG Yang-Heng(郑阳恒)[1] XIE Yi-Gang(谢一冈)[1,3]
LÜ Jun-Guang(吕军光)[3] ZHOU Li(周莉)[3] YU Bo-Xiang(俞伯祥)[3]
ZHANG Ai-Wu(章爱武)[3] AN Zheng-Hua(安正华)[3] XIE Yu-Guang(谢宇广)[3]
ZHANG Dong(张东)[4] ZHENG Zhi-Peng(郑志鹏)[3]

[1] Graduate University of Chinese Academy of Sciences, Beijing 100049, China
[2] Guangxi University, Naning 530004, China
[3] Institute of High Energy Physics, Chinese Academy of Sciences, Beijing 100049, China
[4] Beijing Nuclear Instrument Factory, Beijing 100176, China

Abstract: The THGEM detector without and with a CsI has been tested successfully. The optimal parameters of THGEM have been determined from eight samples. The UV photoelectric effect of the CsI photocathode is observed. The changing tendency related to the extraction efficiency ($\varepsilon_{\rm extr}$) versus the extraction electric field is measured, and several electric fields influencing the anode current are adjusted to adapt to the THGEM detector with a reflective CsI photocathode.

Key words: THGEM, CsI, photocathode, UV

PACS: 29.40.Cs, 95.55.Aq **DOI:** 10.1088/1674-1137/35/4/008

1 Introduction

THick Gaseous Electron Multiplier (THGEM) [1], being a geometrical expansion of the general GEM, is more robust, cheaper and easier to manufacture, and it can reach higher gain than the traditional GEM. It operates on gas multiplication within sub-millimeter diameter holes, in a standard copper-clad printed circuit board (PCB). Recently, numerous studies and applications of THGEM have been processing both inside and outside the field of particle physics [2–4]. CsI is one of the best-known photocathodes for the UV range in high energy physics experiments [5]. It is chemically stable and can be exposed to ambient air for a few tens of minutes without noticeable degradation. Furthermore, it has high absolute quantum efficiency (QE), of the order of 40% at 150nm, in a reflective mode [6]. The CsI reflective photocathode combined with THGEM has recently been shown to be easily produced, has high QE and allows for high gain operation in noble gas mixtures. This established the foundation for designing large area position sensitive gaseous avalanche photomultipliers (GPMT), which have single photon sensitivity and can be used for high precision imaging [7].

In this work, we present some preliminary results of recent investigations of the THGEM detector operation parameters and the effects of associated CsI reflective photocathodes, for possible use as Cherenkov UV photo imaging [8] and X-ray imaging [9], etc.

This paper is organized into two main sections: the first concerns optimizing the characteristics of the THGEM detector; and the second involves the detector with CsI.

2 Optimization of the single THGEM detector

2.1 The THGEM parameters

The THGEM is made of FR4 glass epoxy substrate, copper-clad on both sides with a standard PCB manufacturing process by precise drilling and

Received 21 July 2010, Revised 6 September 2010
* Supported by National Natural Science Foundation of China (10775181,10775151)
1) E-mail: liuhb@mail.ihep.ac.cn

Cu etching in a local PCB factory.

Based on an investigation of previous work [10–12], four independent sectors are further manufactured in two single THGEM boards (0.5 mm and 1.0 mm thick) with the same production process (Fig. 1), to guarantee four sectors working under the same gas conditions. Each sector with the same active area of 3 cm×4 cm is drilled with holes of various diameters: 300 μm, 400 μm, 500 μm, 600 μm, respectively. All holes on the four sectors have the same rim of 100 μm and pitch of 1 mm. The related parameters for eight samples are listed in Table 1.

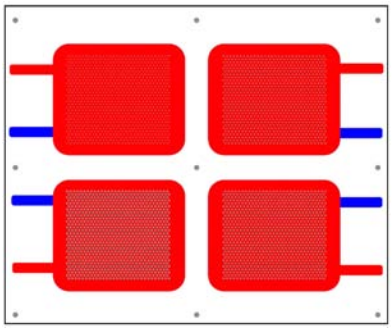

Fig. 1. Schematic diagram of the THGEM with four sectors.

Table 1. THGEMs with various parameters.

THGEM	thickness t/mm	hole diameter d/μm
1#	0.5	300
2#	0.5	400
3#	0.5	500
4#	0.5	600
5#	1.0	300
6#	1.0	400
7#	1.0	500
8#	1.0	600

2.2 Characteristics measurement of single THGEM detector

Figure 2 provides a schematic view of the detector configuration consisting of a cathode, an anode and a single THGEM in between.

The ^{55}Fe X-ray is used as the radioactive source in the case without CsI (in the case with CsI and a deuterium lamp, see Section 3). Ionization is produced in the upper drift region by a 5.3 keV photoelectron generated by the interaction of an ^{55}Fe 5.9 keV X-ray with an Ar atom [13]. The ionized electrons are amplified as an avalanche in the THGEM holes and then enter the lower inductive region, and finally they are collected by the anode.

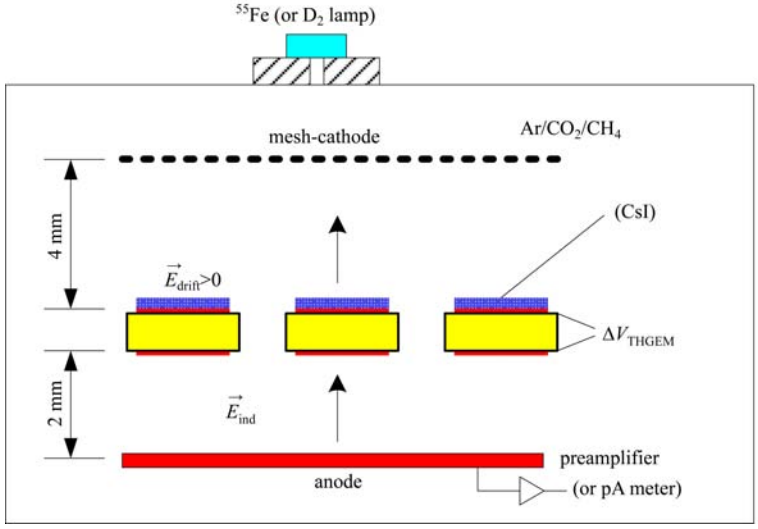

Fig. 2. Schematic diagram of the single-THGEM detector in counting mode (or in current mode).

All electrodes are biased with CAEN SY127 HV power supplies and the signals are recorded in pulse-counting mode with an ORTEC 142 preamplifier (charge sensitivity 1 V/pC) followed by an ORTEC 450 amplifier (shaping time $\tau = 0.5$ μs) and an ORTEC 916 multi-channel analyzer. The THGEM is mounted on a polyethylene (PE) frame and installed in a gas-tight epoxy-made chamber, which is continuously flushed with 1 atm of pre-mixed gas Ar/ CO_2/ CH_4(89/10/1).

By using this calibrated system, the absolute gain for eight kinds of THGEM is obtained, as shown in Fig. 3.

From the eight kinds of THGEM in two groups,

we can find that the thick group working voltage is much higher than the thin group to obtain the same gain. For the thin group, the gain is rather low for the large holes. The gain of the THGEM increases exponentially with the voltage.

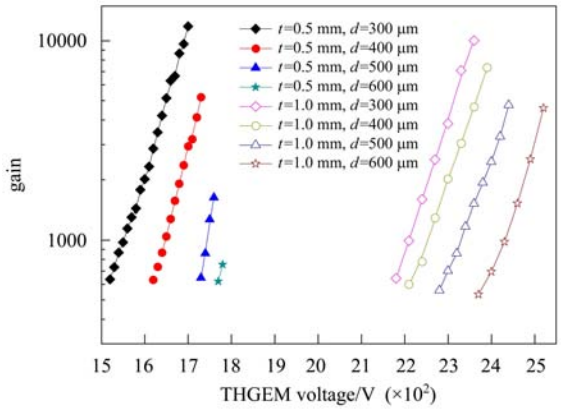

Fig. 3. Gain as a function of the THGEM voltage $\Delta V_{\mathrm{THGEM}}$, measured with a 5.9 keV X-ray in different configurations [THGEM thickness $t = 0.5$ mm (solid symbol), $t = 1.0$ mm (open symbol) and THGEM hole diameter $d = 300$ μm (rhombus), $d = 400$ μm (circle), $d = 500$ μm (triangle), $d = 600$ μm (star)].

The THGEM with a large hole size operates at the higher voltage and increases the possibility of the breakdown, which is mainly triggered by the hole imperfections, Cu burr around the rim and dielectric polarization of the FR4 substrate, etc., and thus could not reach the higher gain.

In addition, the THGEM with a smaller hole size provides a larger sensitive area of the reflective photocathode.

As a detector, the THGEM without CsI, the maximum gain reaches 10^4, and the energy resolution measured from the full-energy peak of ^{55}Fe is around 28% to 60%, which satisfies the application of X-rays, charged particles as well as neutrons with a converter.

3 Experimental study of the performance of the THGEM with a CsI reflective photocathode

The working process of the THGEM with a CsI reflective photocathode can be described as follows. The photocathode, hit by the UV photos, emits photoelectrons into the gas near the top face electrode of the THGEM. These photoelectrons are pulled into the holes, amplified by the gas avalanche under high electric field, and collected on the readout anode.

The effective photon detection efficiency ($\varepsilon_{\mathrm{eff}}$) of the CsI coated THGEM is determined by the QE of CsI photocathode in vacuum ($\mathrm{QE}_{\mathrm{vac}}$), the effective photocathode area (A_{eff}), the efficiency of photoelectron extraction from CsI photocathode in gas ($\varepsilon_{\mathrm{extr}}$) and the photoelectron collection efficiency into the THGEM holes ($\varepsilon_{\mathrm{coll}}$) [14].

$$\varepsilon_{\mathrm{eff}} = \mathrm{QE}_{\mathrm{vac}} \times A_{\mathrm{eff}} \times \varepsilon_{\mathrm{extr}} \times \varepsilon_{\mathrm{coll}}. \quad (1)$$

As a photon detector, the charge on anode output is the crucial point, which is mainly influenced by the drift field , $\Delta V_{\mathrm{THGEM}}$ and inductive field, among which the drift field, $\Delta V_{\mathrm{THGEM}}$ influences the $\varepsilon_{\mathrm{extr}}$ and $\varepsilon_{\mathrm{coll}}$; $\Delta V_{\mathrm{THGEM}}$ determines the avalanche; the inductive field influences the electron clusters collection on anode. Here, we concentrate on the last two factors in Eq. (1), which are effected by the electric fields.

3.1 Influence of extraction field over $\varepsilon_{\mathrm{extr}}$

In order to research the extractive effect of photoelectron ($\varepsilon_{\mathrm{extr}}$) from CsI, two electrodes, the top face of THGEM and the mesh, as shown in Fig. 2, act as a parallel plate configuration. The extracted photoelectrons from CsI are collected by the mesh and recorded in current mode with a Keithley 6485 picoammeter.

The reflective CsI photocathode (170 nm thick) is deposited by thermal evaporation on the THGEM. It is irradiated with UV photons from a continuously emitting deuterium lamp (Mikropack DH-2000-BAL) whose wavelength is estimated to be from 200 nm to 380 nm.

The photocurrent is related to two respects: first, the surface effect including the work function of CsI photocathode, roughness of surface [15]; second, the photoelectron transfer in the the drift region, recombination, attachment and penning effect and so on.

The photocurrent of the CsI photocathode versus the electric field E is shown in Fig. 4, which mainly

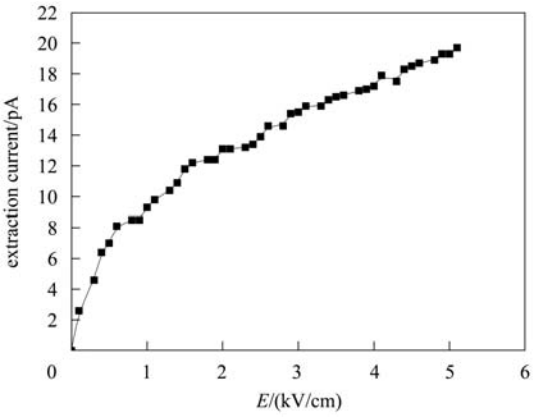

Fig. 4. The measured photoelectron extraction current vs. the electric field.

describes the changing tendency related to the extraction efficiency vs. E. Under the same layout conditions only without coated CsI, the measured photocurrent known as the background current is almost zero.

3.2 Photon detected efficiency of the CsI-coated THGEM

The part of photon detected efficiency, $\varepsilon_{\rm extr}\times\varepsilon_{\rm coll}$ in Eq. (1) depends on $E_{\rm drift}$ and $\Delta V_{\rm THGEM}$.

In order to evaluate the influence of the $E_{\rm drift}$ and $\Delta V_{\rm THGEM}$ over the photoelectron extraction ($\varepsilon_{\rm extr}$) and the electron collection efficiency ($\varepsilon_{\rm coll}$), the electric field induction gap $E_{\rm ind}$ is kept to constant (4 kV/cm) to clarify that the anode current only depends on the $E_{\rm drift}$ and $\Delta V_{\rm THGEM}$.

As illustrated in Fig. 5, the electric field $E_{\rm drift}$ in the detector is varied from −3kV/cm to +3kV/cm in the photocathode gap, and the $\Delta V_{\rm THGEM}$ is set to three different voltages.

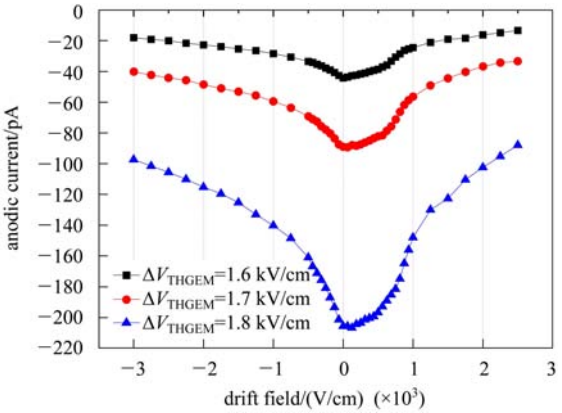

Fig. 5. Anodic current in the THGEM detector vs. $E_{\rm drift}$.

The anode current varies rapidly along with the drift field, which presents a V shape and reaches a maximum at $E_{\rm drift}$=0. The three curves with different $\Delta V_{\rm THGEM}$ show obviously the avalanche development in the THGEM holes. The THGEM with reflective CsI photocathode works properly.

The maximum photon detection efficiency is obtained at $E_{\rm drift}$=0, which is different from the semitransparent CsI photocathode THGEM. A slightly reversed $E_{\rm drift}$ (is consistent with the result 50–100 V/cm in Ref. [16]) could make the gas-ionized electrons in the drift gap drift back to the mesh electrode, thus makes the detector practically blind to the gas ionization.

We note that the electric field in the drift gap affects the anodic current in two main competitive physical processes: $E_{\rm drift}<0$ increases the photoelectron emitting probability from the photocathode surface ($\varepsilon_{\rm extr}$ increase), however, it causes the photoelectron transferring toward the mesh instead of entering the THGEM aperture ($\varepsilon_{\rm coll}$ decrease); whereas, the positive external field, $E_{\rm drift}>0$, results in a higher electron collection efficiency ($\varepsilon_{\rm coll}$ increase) through THGEM, but a lower photoelectron extraction ($\varepsilon_{\rm extr}$ decrease) due to low electric field.

It gives us a clear indication to optimize the reflective CsI photocathode THGEM detector design.

The effective photon detection efficiency mentioned above is the relative efficiency. In this measurement, the UV light source (200–380 nm) is just near the long wavelength cutoff edge of the CsI spectral sensitive region (around 210 nm), which causes a low QE measurement compared with the UV PMT. As to the measurement of the absolute efficiency, some extra devices are needed, such as a calibrated CsI photocathode PMT (Hamamatsu R6835), an MWPC with known efficiency, etc.

4 Conclusion and discussion

The THGEM detector without and with CsI has been built and tested successfully, and the optimal parameters of THGEM, as the main component of the detector, have been determined from eight samples.

The thin THGEM with small holes can work at a relatively low voltage with high gain and high stability. The THGEM with thickness $t=0.5$ mm and hole diameter $d=300$ μm is an optimized choice for the reflective photocathode due to its larger photo sensitive area.

The changing tendency related to the extraction efficiency ($\varepsilon_{\rm extr}$) versus the extraction electric field is measured, and several electric fields influencing the anode current are adjusted to adapt to the THGEM detector with a reflective CsI photocathode.

The photoelectron transfer effect of CsI-coated THGEM reaches the maximum when $E_{\rm drift}$ is close to zero, which is different from the semitransparent CsI photocathode THGEM and gas ionization THGEM detector. A slightly reversed $E_{\rm drift}$ could make the detector practically blind to the gas ionization.

The relative QE of the CsI photocathode is expected to be improved by optimizing some detector parameters, such as the CsI film thickness and vacuum thermal evaporation process.

We would like to express our sincere appreciation to A. Breskin of Weizmann Inst., P. Picchi and A. Braem of CERN for their friendly discussions and kind support. Many thanks also go to the NNSF of China for support of this work.

References

1 Chechik R, Breskin A, Shalem C et al. Nucl. Instrum. Methods A, 2004, **535**: 303–308
2 Chechik R, Breskin A, Shalem C. Nucl. Instrum. Methods A, 2005, **553**: 35–40
3 Hanu A, Byuna S H, Prestwich W V. Nucl. Instrum. Methods A, 2010,doi:10.1016/j.nima.2010.07.033
4 Boccone V. J. Phys.: Conf. Ser. 2009, 160 012032
5 Breskin A. Nucl. Instrum. Methods A, 1996, **371**: 116–136
6 Shefer E, Singh B K. Nucl. Instrum. Methods A, 2000, **442**: 58–67
7 Mörmanna D, Breskin A, Chechik R et al. Nucl. Instrum. Methods A, 2002, **478**: 230–234
8 Alexeev M et al. Nucl. Instrum. Methods A, 2009, doi:10.1016/j.nima.2009.08.087
9 Cortesi M, Alon R, Chechik R et al. 2007 JINST 2 P09002
10 An Z H et al. CPC(HEP & NP), 2010, **34(1)**: 83–87
11 Shalem C et al. Nucl. Instrum. Methods A, 2006, **558**: 475–489
12 Shalem C K et al. Nucl. Instrum. Methods A, 2006, **558**: 468–474
13 XIE Y G, CHEN C et al. Particle Detector and Data Acquisition. Beijing: Science Press, 2003. 20 and 628 (in Chinese)
14 Azevedo C D R et al. JINST, 2010, **5**: P01002
15 Nitti M A,Nappi E et al. Nucl. Instrum. Methods A, 2005, **553**: 157–164
16 Breskin A. Talk in RD51 4th Coll. Meeting, Nov. 24, 2009